OPTIMIZATION DESIGN OF SOUND BARRIER WITH ABSORBING MATERIAL USING TOPOLOGY OPTIMIZATION

Leilei Chen
Xinyang Normal University, College of Architecture and Civil Engineering, Xinyang, Henan, China
email: chenllei@mail.ustc.edu.cn

Wenchang Zhao
University of Science and Technology of China, Department of Modern Mechanics, Hefei, China

A topology optimization approach based on the boundary element method (BEM) and the optimality criteria (OC) method is proposed for the optimal design of sound absorbing material distribution within sound barrier structures. The acoustical effect of the absorbing material is simplified as the acoustical admittance boundary condition. Based on the solid isotropic material with penalization (SIMP) method, a topology optimization model is established by selecting the densities of absorbing material elements as design variables, volume of absorbing material as constraints, and the minimization of sound pressure at reference surface as design objective. A smoothed Heaviside-like function is proposed to help SIMP obtain a clear 0–1 distribution. The BEM is applied for acoustic analysis and the sensitivities with respect to design variables are obtained by the direct differentiation method. The Burton–Miller formulation is used to overcome the fictitious eigen-frequency problem for exterior boundary-value problems. A relaxed form of OC is used for solving the optimization problem to find the optimum absorbing material distribution. Numerical examples are provided to illustrate the application of the topology optimization for 2D sound barriers. Results show that the optimal distribution of the sound absorbing material is strongly frequency dependent, and performing an optimization in a frequency band is generally needed.

Keywords: Topology optimization, Boundary element method, Solid isotropic material with penalization, Absorbing material

1. Introduction

Sound barriers have been widely applied for transportation noise reduction, and many researchers have conducted performance evaluations of sound barrier by various numerical methods. Among these methods, the boundary element method (BEM) outperforms the others for the acoustic analysis of sound barrier because of its capability to provide excellent accuracy and easy mesh generation. Moreover, the Sommerfeld radiation condition at infinity is automatically satisfied for exterior acoustic problems. Ishizuka and Fujiwara [1] evaluated the performance of different types of sound barrier with various shapes and acoustical conditions by BEM. Their results show that the absorbing edges significantly improve the barrier efficiency. Monazzam and Lam [2] presented an investigation about the acoustic performance of sound barriers with quadratic residue diffuser tops by a 2D BEM. Thus, the BEM is selected in the current work for the acoustic analysis of barriers.

Optimizations in sound barriers have also been investigated by many researchers to improve the performance of sound barriers. However, most of the previous works focused on the shape design of sound barrier but few researchers investigated the optimization for absorbing materials or acoustical conditions. This paper presents a topology optimization approach for the optimal design of absorbing material distribution within sound barriers. Solid isotropic material with penalization (SIMP) is a popular method of topology optimizations and has been applied to a range of topology optimization problems due to its computational efficiency and conceptual simplicity. The SIMP approach converts discrete values into continuous variables, and suppresses the intermediate densities by penalization. However, gray elements cannot be precluded completely through a penalization scheme, and several methods are thus applied for the gray element elimination. In the present work, a SIMP-based interpolation scheme is used to convert the original discrete optimization problem into a nonlinear programming problem. An operator is used to help SIMP sharpen intermediate values to obtain a clear 0-1 distribution. A relaxed form of the OC method is selected to solve the problem. The OC method is suitable for problems with a large number of design variables but with one constraint.

2. Optimization model based on the BEM

2.1 Optimization model

The discretized optimization model is formulated as follows:

$$\begin{cases} \min & \Pi = \overline{\mathbf{p}}_f \mathbf{p}_f \\ \text{s.t.} & \sum_{i=1}^{n} \rho_i v_i - V_0 \leqslant 0 \\ & 0 \leqslant \rho_{\min} \leqslant \rho_i \leqslant 1 \end{cases} \tag{1}$$

where $\mathbf{p}_f$ denotes the sound pressure vector in field points located on a prescribed reference plane, and $\overline{\mathbf{p}}_f$ denotes the conjugate transpose of $\mathbf{p}_f$. ρ_i and v_i denote volumetric density and volume of element i $(i = 1, 2, \ldots, n)$ respectively, $\rho_{\min}$ is the lower bound of volumetric density to avoid singular value, and V_0 denotes the constraint function. $\mathbf{p}_f$ can be obtained by the following integral equation:

$$\mathbf{p}_f = -[\mathbf{H}_1 - ik\mathbf{G}_1\mathbf{B}]\mathbf{p} + \mathbf{p_i} \tag{2}$$

where the matrices $\mathbf{H}_1$ and $\mathbf{G}_1$ are similar to the coefficient matrices in BEM, but the source nodes are located at the exterior acoustic domain. And $\mathbf{B}$ is defined by

$$\mathbf{B} = \begin{bmatrix} \beta_1 & & \\ & \ddots & \\ & & \beta_n \end{bmatrix} \tag{3}$$

By differentiating $\mathbf{p}_f$ with respect to the design variables, the following formulation can be obtained:

$$\begin{aligned} \frac{\partial \mathbf{p}_f}{\partial \rho_i} = & - \left[\mathbf{H}_1 - ik\mathbf{G}_1\mathbf{B}\right]\left[\mathbf{H} - ik\mathbf{G}\mathbf{B}\right]^{-1}\left[ik\mathbf{G}\frac{\partial \mathbf{B}}{\partial \rho_i}\right]\mathbf{p} \\ & + \left[ik\mathbf{G}_1\frac{\partial \mathbf{B}}{\partial \rho_i}\mathbf{p}\right] \end{aligned} \tag{4}$$

where the matrices $\mathbf{H}$ and $\mathbf{G}$ are the coefficient matrices in BEM.

The sensitivities of the objective function in Eq. (1) can be expressed as:

$$\frac{\partial \Pi}{\partial \rho_i} = \frac{\partial \left(\overline{\mathbf{p}}_f \mathbf{p}_f\right)}{\partial \rho_i} = 2\Re\left(\overline{\mathbf{p}}_f \frac{\partial \mathbf{p}_f}{\partial \rho_i}\right) \tag{5}$$

where $\Re$ denotes the real part of the complex value. By substituting Eqs. (2) and (4) into Eq. (5), the sensitivities of objective function with respect to design variables can be obtained. The sensitivities in Eq. (5) are filtered by the Sigmund filter to avoid checkerboard and mesh-dependency problems.

2.2 Material interpolation scheme

The original optimization problem with discrete 0–1 design variables is difficult to solve mathematically, and this difficulty can be overcome by converting discrete variables into continuous values using a continuous interpolation function. The use of sound absorbing material changes the normalized surface admittance. For the void element without absorbing material, β is 0; for the solid element fully covered with sound absorbing material, β is set to 1 for simplicity, marked as β_0. We assuming that the relation between the normalized surface admittance and the material density at element i can be expressed as:

$$\beta_i = \beta_0 f(\rho_i) \tag{6}$$

We introduce the SIMP interpolation function as

$$f(\rho_i) = \rho_i^p \tag{7}$$

where p is the penalization factor, generally $p \geqslant 3$, thereby making the intermediate density approach either 0 (void) or 1 (solid). Figure 1 shows the penalization performance of different p values. It can be seen that larger p induce sharper changes near the right end. The value of p may influence the efficiency and final solution of the optimization procedure, and will be investigated in the following numerical examples.

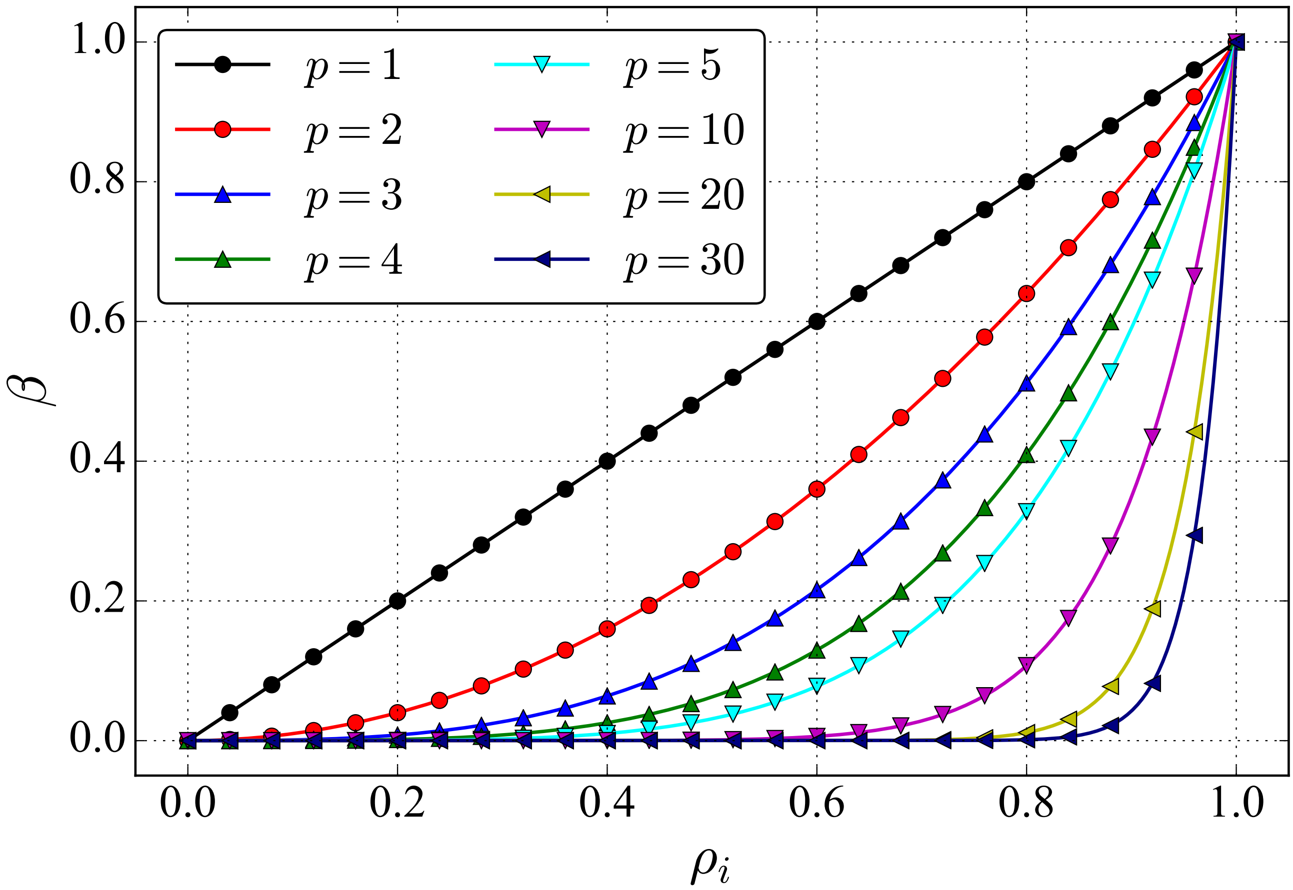

Figure 1: Penalization performance of different p values for SIMP interpolation scheme.

3. Numerical examples

3.1 Problem description

The topology optimization procedure is implemented in a self-programming Fortran 90 program. The following examples are computed in a PC with an Intel Core i7 CPU and 16 GB memory.

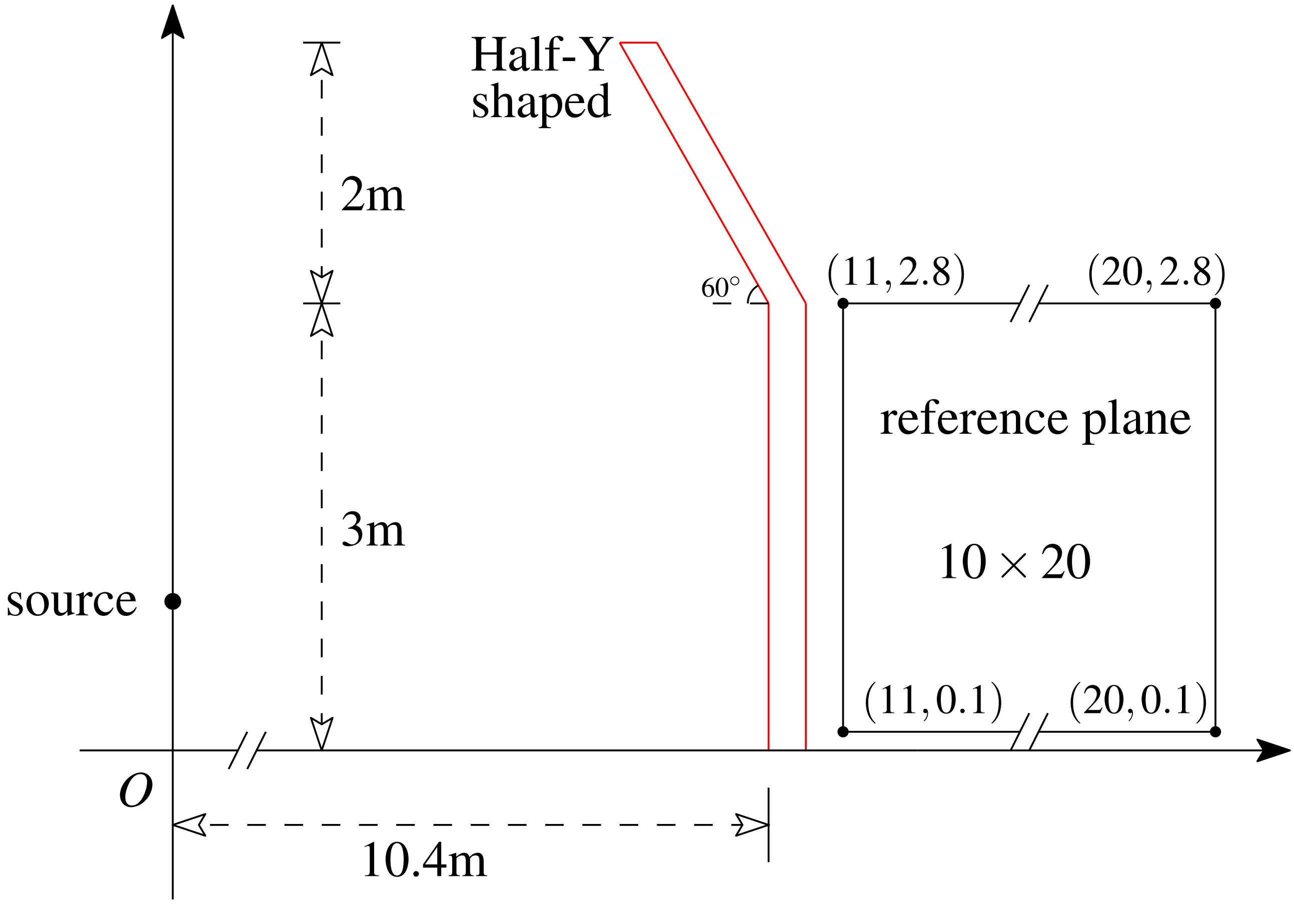

Figure 2: Half-Y-shaped and plain sound barrier.

To investigate the validity and applicability of the developed optimization procedure, we consider the analysis and design domain of a half-Y-shaped sound barrier in Fig. 2. A unit point source is located at $(0, 1)$ m, and the excitation frequency of the source is set as 100 Hz. In following examples, $\rho_{\min}$ is set as 10^{-3}, and the iterative convergence criterion τ is set as 10^{-4}.

3.2 Insert loss at 100 Hz

we introduce the insertion loss to evaluate the barrier performance

$$IL = 20 \log_{10} \left| \frac{p_2}{p_1} \right| \tag{8}$$

where p_1 and p_2 are the sound pressures at the receiver with and without the barrier, respectively, for the same ground condition and source position. The change in insertion loss, ΔIL, can indicate the performances of different sound barriers.

$$\begin{aligned} \Delta IL_1 &= IL_{\text{Opt}} - IL_{\text{Rigid}} \\ \Delta IL_2 &= IL_{\text{Opt}} - IL_{\text{Full}} \end{aligned} \tag{9}$$

where the subscripts "Opt", "Rigid" and "Full" denote the layouts after optimization, with no covering and with fully covering, respectively.

Figure 3 shows the $\Delta IL_i (i = 1, 2)$ contour plots of a half-Y-shaped sound barrier; subfigure (a) is ΔIL_1, and subfigure (b) is ΔIL_2. Figure (a) compares the insert losses of Half-Y-shaped barriers with "Opt" and "Rigid" absorbing material layouts. From this figure, the "Opt" layout produces approximately a 5–10 dB increase in IL over the "Rigid" layout at the reference surface, and the increase is approximately 0–5 dB in the major area behind the barrier. Hence, using absorbing material is beneficial to improve the noise reduction of sound barrier. Figure (b) compares the insert losses with "Opt" and "Full" absorbing material layouts. From this figure, considerable increment in IL, i.e. the ΔIL_2, is observed at the reference surface of the barrier. The performance of "Opt" layout is superior to the "Full" layout, although the former consumes less absorbing material than the latter. In general, using absorbing material contributes to the performance of sound barrier. However, the layout with full covering of absorbing material does not perform the best.

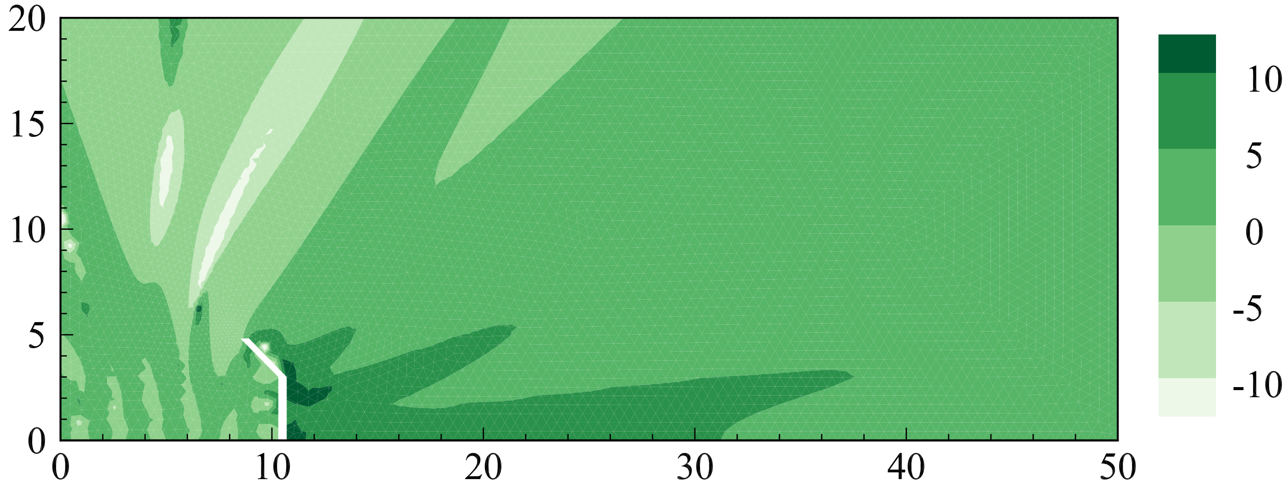

(a)

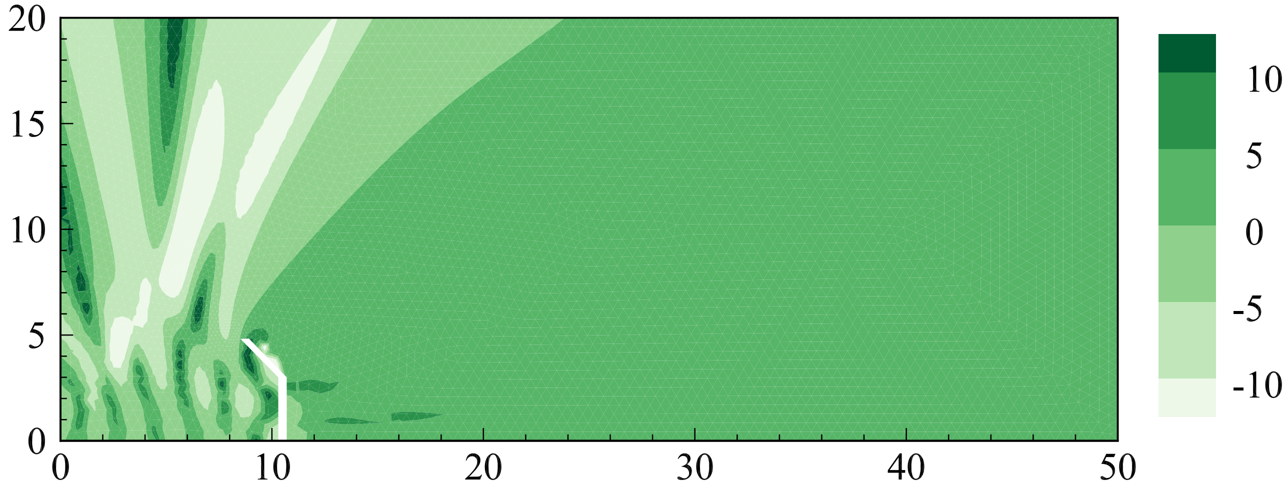

(b)

Figure 3: ΔIL_1 and ΔIL_2 contour plots of a half-Y-shaped sound barrier: (a) ΔIL_1; (b) ΔIL_2.

4. Conclusion

This study investigates the SIMP-based topology optimization for the sound absorbing material distribution within sound barriers. A smoothed Heaviside-like function is used to help SIMP exclude the gray element effectively for a sharp 0–1 distribution, and a relaxed form of OC is adopted to obtain the solution to the optimization model. Numerical examples are used to demonstrate the validity of the proposed approach and necessity for optimal design. The simulation results show that using absorbing material helps improve the performance of a sound barrier, but a sound barrier fully covered with absorbing material may not be the best selection. The proposed optimization procedure is able to provide a proper absorbing material distribution under material volume constraints. The optimal distribution is strongly frequency and frequency band dependent, and it shows a more complicated distribution as excitation frequency or considered frequency band increases. Comparisons of optimal distributions with and without gray element elimination show that the proposed function is able to exclude the gray element effectively.

Acknowledgements

Financial supports from the China Scholarship Council (CSC), National Natural Science Foundation of China (NSFC) under Grant no. 11172291, and Research Fund for the Doctoral Program of Higher Education of China under Grant no. 20133402110036.

REFERENCES

1. Fujiwara, K., Hothersall, D.C., Hwan Kim, C. Noise barriers with reactive surfaces, *Applied Acoustics*, **53** (4), 255–272, (1998).

2. Monazzam, M., Lam, Y. Performance of profiled single noise barriers covered with quadratic residue diffusers, *Applied Acoustics*, **65** (2), 125–141, (2010).